ANNALS OF COMMUNICATIONS IN MATHEMATICS
Volume 8, Number 1 (2025), 1-27
DOI: 10.62072/acm.2025.080101
ISSN: 2582-0818
https://www.technoskypub.com/journal/acm/

VECTOR CONTROL STRATEGIES AND A QUANTITATIVE PARTIAL DIFFERENTIAL EQUATIONS APPROACH OF SPATIAL MATHEMATICAL MODEL ON MALARIA TRANSMISSION DYNAMICS

CHARITY JUMAI ALHASSAN* AND KENNETH OJOTOGBA ACHEMA

ABSTRACT. A spatial mathematical model to study the impact of vector control strategies on the dynamics of malaria transmission and its analysis is considered in this paper. The resulting model equations are divided into homogeneous and non-homogeneous equations. The homogeneous equations are solved to determine their disease-free equilibrium (DFE) and their stability. A basic reproduction number was determined from the DFE. It was found that when basic reproduction number is less one, the disease will die out, when the basic reproduction number is exactly one, the model undergoes a backward bifurcation, when the basic reproduction number is exactly zero, the model undergoes forward bifurcation and whenever the basic reproduction is greater than one, the disease will persist in the population. A quantitative sensitivity analysis of the model parameters was also conducted through the disease's basic reproduction number to determine the parameters that are sensitive to malaria transmission. A travelling wave equation and solutions were also provided for a possible understanding of the behaviour of mosquitoes' mobility in the human environment. Finally, we carried out a simulation of our formulated partial differential model and quantitatively assessed and investigated the twin effect of the presence of invasive plants and the spatial dispersion of vectors on malaria dynamics. Sensitivity analysis was also carried out, and the quantitative effect of diffusion and advection on the wave front was demonstrated. The speed of the disease propagation by using travelling wave solutions of the model was also investigated numerically.

1. INTRODUCTION

The Malaria Control Strategy Agenda using Dichlorodiphenyltrichloroethane (DDT), which became the main tool for the World Health Organisation (WHO) malaria eradication programme from 1956–1967, fell out because of its effects on environmental management. Since the failure of this campaign to sustainably eliminate malaria from the tropics, the effectiveness of environmental management has remained poorly explored. Changes in invasive plant structure and composition, whether due to deforestation or to due land use

2020 *Mathematics Subject Classification.* 35-XX, 35CXX, 35C07.
Key words and phrases. Partial differential equations; Travelling wave; Equilibrium; Stability.
Received: December 12, 2024. Accepted: March 07, 2025. Published: March 31, 2025.

*Corresponding author.

changes were carefully studied [28]. [28]proposed modern vector control strategies, such as invasive plant control and the control of vectors, which will significantly reduce vector proliferation and the spatial dynamics of vectors on the dynamics of malaria within a given habitat [2].

Mosquitoes, including invasive species (this species has spread to many countries through the transport of goods and international travel), such as the Asian tiger mosquito Aedes albopictus, alongside the native species Culex pipiens s.l., pose a significant nuisance to humans and serve as vectors for mosquito-borne diseases in urban areas. Understanding the impact of water infrastructure characteristics, climatic conditions, and management strategies on mosquito occurrence and the effectiveness of control measures to assess their implications for mosquito occurrence is crucial for effective vector control.

Currently, few studies have linked ecological drivers to changes in mosquito populations within urban environments, often resulting in contradictory conclusions. Some studies have proposed that alterations in top-down ecological dynamics may lead certain mosquito species to dominate urban areas due to reduced predation pressures [2, 13]. Conversely, other research suggests that increasing levels of urban pollution can reduce the quality of larval habitats, thereby promoting the dominance of genera such as Culex, which are known for their adaptability to temporary and degraded aquatic habitats and invasive alien plants [13, 28]. Consequently, the epidemiology of mosquito-borne diseases can be significantly impacted [12], resulting in severe outbreaks of diverse mosquito-borne pathogens such as malaria, even in regions previously considered non-endemic. Additionally, this situation elevates the risk of the introduction and reintroduction of emerging infectious diseases [15].

Among the most abundant mosquitoes in urban areas, invasive species such as the Asian tiger mosquito Ae. albopictus are of great concern because they cause nuisance and pose a global health risk [14, 21]. The economic implications of their presence are also significant [17]. While Ae. albopictus is native to Southeast Asia and is typically found in natural habitats such as bamboo stumps, invasive alien plants, tree holes, discarded tires, and flower vases [27, 28], its range has expanded globally [20], becoming more common in urban areas. The spread of Ae. albopictus has been facilitated through the trade of ornamental plants and used tires over long distances [3], as well as passive transportation in cars over shorter distances [13]. Urbanisation processes also favour the proliferation of Ae. albopictus populations [26]. In Catalonia (northeast Spain), Ae. albopictus was first identified as an invasive species in 2004, with the first records of its presence in the province of Barcelona [7] and in the city itself since 2005 [31]. This species has suitable conditions for reproduction along the entire eastern coast of Spain [3].

Although mosquito-borne diseases are significant public health concerns, particularly in urban environments, it is crucial to understand how ecological drivers affect the population dynamics of mosquito species such as Ae. albopictus and Cx. pipiens to develop effective management strategies to mitigate their spread.

Mathematical models for the transmission dynamics of malaria are useful for providing better insights into the behavior of the disease. These models have played important roles in influencing decision-making processes regarding intervention strategies for preventing and controlling malaria. The study of malaria using mathematical modelling began in 1911 [10]. He introduced the first deterministic two-dimensional model with one variable representing human and the other representing mosquitoes, where it was shown that a reduction in the mosquito population below a certain threshold was sufficient to eradicate malaria. In [29], Ross's model was modified by considering the latency period of the parasites

in mosquitoes and their survival during that period. However, in this case, reducing the number of mosquitoes is an inefficient control strategy that would have little effect on the epidemiology of malaria in areas of intense transmission. Further extension was described by [5], where the latency of infection in humans was introduced by making the additional exposed class in humans. This modification further reduces the long-term prevalence of both infected humans and infected mosquitoes.

Thus, all other models that exist for malaria dynamics are developed from the three basic models explained earlier by incorporating different factors to make them biologically more realistic in explaining disease prevalence and prediction [29]. For example, a number of epidemiological studies [8, 19, 23, 1, 4] have considered the inclusion of the recovered class, which incorporates time-dependent immunity that develops during recovery from infection in humans. Further work on acquired immunity in malaria has been conducted by [9]. Their models take into account that acquired immunity to malaria depends on continuous exposure to reinfection. Moreover, some models have integrated other factors, such as environmental effects[16, 33], mosquito resistance to insecticides and resistance of some parasite strains to anti-malaria drugs [34].

The incidence rate is of utmost importance in the transmission dynamics of the disease, as the qualitative behaviour of the disease depends on it. The incidence of malaria infection is referred to as the number of new infected individuals (humans or mosquitoes) yielding in unit time. The most commonly used incidence rates in the formulation of models for malaria transmission are simple mass-action and standard incidences. For other forms of incidence functions that arise in epidemiological models [18].

The model presented in this paper is subdivided into eight compartments, which include four compartments in humans, one compartment in invasive alien plants and three compartments in mosquitoes, with inclusions of non-linear forces of infection in both the host and vector populations. The disease-induced death rates for humans and mosquitoes were also incorporated into the model assumed to be the same as the recruitment rates for humans and mosquitoes, while the rates for invasive alien plants followed the logistic model equation.

The remainder of this paper is organised as follows: we provide a full description of the model in Section 2. In Section 3, we provide the existence of equilibria, including a derivation of the basic reproduction number and a stability analysis of the equilibria and backwards bifurcation results. Section 4 provides numerical simulations of the model with graphical illustrations with specific interest in the PDE model. In Section 5, we formulated and carry out a travelling wave equations analysis and simulations. Finally, we discuss and conclude in Section 6 and Section 7 respectively.

2. Model Formulation

In this section, we provide assumptions of the model,and describe the model variables and parameters,and the model flow or schematic diagram that will enhance quick understanding our formulation system of equations.

2.1. **Assumptions of the model equations.**

For proper understanding and formulation of system of equations in this study, we present the following assumptions:

- (A_{α_1}) Mosquitoes migrate from vegetation/invasive plants to the human population due to their proximity to human habitat [24].
- (A_{α_2}) To make the population constant over time, we assumed that the recruitment rate is the same as those that died naturally and due to infection[33].

(A_{α_3}) We also assume that recovered humans lost immunity and became susceptible.
(A_{α_4}) We assumed a spatial movement of vectors from the invasive plants sites at the borders of the community;
(A_{α_5}) We assumed that the distance measures from where the invasive plants are to human habitat can be covered by the vectors (Anopheles mosquitoes)[24]
(A_{α_6}) We consider that susceptible, exposed and infected vectors have the same coefficients of diffusion, D and of advection, K, because the disease has no effect on vector movement [33].
(A_{α_7}) Invasive plants close to the human population is capable of providing shelter for a high density of the mosquito population.

2.2. **Model variables and parameters.** The variables and the parameters of our formulated model are given as Table 1 and Table 2 respectively as follows.

Variable/Parameter	Interpretation
$S_h(t)$	Number of susceptible human at time t
$E_h(t)$	Number of exposed humans at time t
$I_h(t)$	Number of infected humans at time t
$R_h(t)$	Number of recovered humans at time t
$P(t)$	Invasive Plants population
$S_m(t)$	Number of susceptible mosquitoes at time t
$E_m(t)$	Number of Exposed mosquitoes at time t
$I_m(t)$	Number of infected mosquitoes at time t
b	Number of bite per mosquito/vector
D	The coefficient of diffusion
K	The coefficient of advection
q_h	Rate at which exposed human population become infected
v_h	Recovered rate of infected individual
α_h	Recovery rate of human
h	Control rate of invasive plants
θ_m	recruitment rate of mosquitoes from the density of invasive plants into the general susceptible mosquito
μ_h	Natural death rate of humans
δ_h	Disease induced death rate
g	Growth rate of plant
K_p	Plant carrying capacity
μ_m	Natural death rate of mosquitoes
ξ_m	Death rate of mosquito due to insecticide spray
$\lambda_h(t)$	Force of infection for humans
$\lambda_m(t)$	Force of infection for vectors
β_{hv}	probability of malaria from infectious humans to susceptible mosquitoes
β_{mh}	probability of malaria from vectors to humans
ϵ	Availability of bed-nets
γ	Efficacy of bed-nets

TABLE 1. Description of model variables and parameters

2.3. **Model flow diagram.** In order to provide easy understanding of the derivation of the system of equations under consideration, we construct eight (8) compartmental flow diagram as shown below.

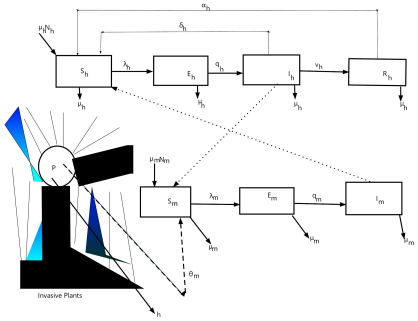

FIGURE 1. Model schematic diagram

2.4. **Model equations.** Following the assumptions, variables and parameters stated above in addition to the schematic diagram, our model equations is stated thus:

$$
\begin{aligned}
\frac{\partial \bar{S_h}}{\partial t} &= \mu_h \bar{N_h} + \delta_h \bar{I_h} + \alpha_h \bar{R_h} - \lambda_h \bar{S_h} - \mu_h \bar{S_h} \\
\frac{\partial \bar{E_h}}{\partial t} &= \lambda_h \bar{S_h} - (q_h + \mu_h)\bar{E_h} \\
\frac{\partial \bar{I_h}}{\partial t} &= q_h \bar{E_h} - (\delta_h + \mu_h + v_h)\bar{I_h} \\
\frac{\partial \bar{R_h}}{\partial t} &= v_h \bar{I_h} - (\mu_h + \alpha_h)\bar{R_h} \\
\frac{\partial \bar{P}}{\partial t} &= g(1 - \frac{\bar{P}}{K_P})\bar{P} - h\bar{P} \\
\frac{\partial \bar{S_m}}{\partial t} &= D\frac{\partial^2 \bar{S_m}}{\partial x^2} - K\frac{\partial \bar{S_m}}{\partial x} + \mu_m \bar{V} + \theta_m P - \lambda_m \bar{S_m} - \mu_m \bar{S_m} \\
\frac{\partial \bar{E_m}}{\partial t} &= D\frac{\partial^2 \bar{E_m}}{\partial x^2} - K\frac{\partial \bar{E_m}}{\partial x} + \lambda_m \bar{S_m} - (q_m + \mu_m)\bar{E_m} \\
\frac{\partial \bar{I_m}}{\partial t} &= D\frac{\partial^2 \bar{I_m}}{\partial x^2} - K\frac{\partial \bar{I_m}}{\partial x} + q_m \bar{E_m} - \mu_m \bar{I_m}
\end{aligned} \tag{1}
$$

Where,

$$
\begin{aligned}
\lambda_h &= (1 - \epsilon\gamma)\beta_{hm}\frac{b\bar{I_m}}{\bar{N_h}}, \\
\lambda_m &= (1 - \epsilon\gamma)\beta_{mh}\frac{b\bar{I_h}}{\bar{N_h}}
\end{aligned} \tag{2}
$$

$$0 < \epsilon < 1, 0 < \gamma < 1$$

with

$$\bar{S_h}(0,x) > 0, \bar{E_h}(0,x) \geq 0, \bar{I_h}(0,x) \geq 0, \bar{R_h}(0,x) \geq 0$$
$$\bar{P}(0,x) \geq 0$$

where D and K are the coefficients of diffusion and advection of the mosquitoes respectively.
The total human population is $\bar{N_h} = \bar{S_h} + \bar{E_h} + \bar{I_h} + \bar{R_h}$.

Substituting the following change of variables
$S_h = \frac{\bar{S_h}}{\bar{N_h}}, E_h = \frac{\bar{E_h}}{\bar{N_h}}, I_h = \frac{\bar{I_h}}{\bar{N_h}}, R_h = \frac{\bar{R_h}}{\bar{N_h}}, P = \frac{\bar{P}}{P^*}, S_m = \frac{\bar{S_m}}{\bar{N_m}}, E_m = \frac{\bar{E_m}}{\bar{N_m}}$ and $I_m = \frac{\bar{I_m}}{\bar{N_m}}$. into Eq. (1), we obtain

$$\begin{aligned}
\frac{\partial S_h}{\partial t} &= \mu_h(1 - S_h) + \delta_h I_h + \alpha_h R_h - k_1 S_h I_m \\
\frac{\partial E_h}{\partial t} &= k_1 S_h I_m - (q_h + \mu_h) E_h \\
\frac{\partial I_h}{\partial t} &= q_h E_h - (\delta_h + \mu_h + v_h) I_h \\
\frac{\partial R_h}{\partial t} &= v_h I_h - (\mu_h + \alpha_h) R_h \\
\frac{\partial P}{\partial t} &= g(1 - P)P - hP \\
\frac{\partial S_m}{\partial t} &= D\frac{\partial^2 S_m}{\partial x^2} - K\frac{\partial S_m}{\partial x} + \mu_m(1 - S_m) + \theta_m c P - k_2 I_h S_m \\
\frac{\partial E_m}{\partial t} &= D\frac{\partial^2 E_m}{\partial x^2} - K\frac{\partial E_m}{\partial x} + k_2 I_h S_m - (q_m + \mu_m) E_m \\
\frac{\partial I_m}{\partial t} &= D\frac{\partial^2 I_m}{\partial x^2} - K\frac{\partial I_m}{\partial x} + q_m E_m - \mu_m I_m
\end{aligned} \tag{3}$$

where

$$\begin{aligned}
k_1 &= (1 - \epsilon\gamma)\beta_{hm} b \frac{\bar{N_m}}{\bar{N_h}}, \\
k_2 &= (1 - \epsilon\gamma)\beta_{mh} b \\
c &= \frac{k_p}{\bar{N_m}} \\
0 < \epsilon < 1, 0 < \gamma < 1
\end{aligned}$$

Now, from the normalization and rescaling carried out, we can now uncouple the system to become:

$$\begin{aligned}
\frac{\partial e_h}{\partial t} &= \lambda_h(1 - e_h - i_h - r_h) - (q_h + \mu_h) e_h \\
\frac{\partial i_h}{\partial t} &= q_h e_h - (\delta_h + v_h + \mu_h) i_h \\
\frac{\partial r_h}{\partial t} &= v_h i_h - (\mu_h + \alpha_h) r_h \\
\frac{\partial e_m}{\partial t} &= D\frac{\partial^2 e_m}{\partial x^2} - K\frac{\partial e_m}{\partial x} + \lambda_m(1 - e_m - i_m) - (q_m + \mu_m) e_m \\
\frac{\partial i_m}{\partial t} &= D\frac{\partial^2 i_m}{\partial x^2} - K\frac{\partial i_m}{\partial x} + q_m e_m - \mu_m e_m
\end{aligned} \tag{4}$$

In order to carry out some qualitative analyses of our formulated model, we decoupled the homogeneous part of Eq. (3) as given by

$$\begin{aligned}
\frac{dS_h}{dt} &= \mu_h(1-S_h) + \delta_h I_h + \alpha_h R_h - k_1 S_h I_m \\
\frac{dE_h}{dt} &= k_1 S_h I_m - (q_h + \mu_h) E_h \\
\frac{dI_h}{dt} &= q_h E_h - (\delta_h + \mu_h + v_h) I_h \\
\frac{d}{dt} &= v_h I_h - (\mu_h + \alpha_h) R_h \\
\frac{dP}{dt} &= g(1-P)P - hP \\
\frac{dS_m}{dt} &= \mu_m(1-S_m) + \theta_m c P - k_2 I_h S_m \\
\frac{dE_m}{dt} &= k_2 I_h S_m - (q_m + \mu_m) E_m \\
\frac{dI_m}{dt} &= q_m E_m - \mu_m I_m
\end{aligned} \tag{5}$$

where

$$\begin{aligned}
k_1 &= (1-\epsilon\gamma)\beta_{hm} b \frac{\bar{N_m}}{\bar{N_h}}, \\
k_2 &= (1-\epsilon\gamma)\beta_{mh} b \\
c &= \frac{k_p}{\bar{N_m}} \\
0 < \epsilon < 1, 0 < \gamma < 1 &
\end{aligned}$$

3. Basic properties of the spatial homogeneous equations

Let $N_h(t) = S_h(t) + E_h(t) + I_h(t) + R_h(t)$ be the total population of human at time, t. Also, let $N_m(t) = S_m(t) + E_m(t) + I_m(t)$ be the total population of mosquitoes at time, t. Let $R_1 = P(t)$ be the plants population at time, t. The feasible region of the model (5) is given by

$\Omega = \{(S_h+E_h+I_h+R_h, P, S_m+E_m+I_m) \in \Re_+^8 : S_h+E_h+I_h+R_h = 1; P = \frac{g}{h}; S_m+E_m+I_m = 1, S_h > 0, E_h \geq 0, I_h \geq 0, R_h \geq 0; P > 0; S_m > 0, E_m \geq 0, I_m \geq 0\}$ is positively invariant.

3.1. **Disease Free Equilibrium (DFE) Analysis.** In this section, we shall carry out a qualitative analysis of the model equations as follows.

3.2. **Case I: When there are invasive plants in human environment.** Disease Free-equilibrium (DFE) corresponding to the presence of invasive plants is given by

$$\begin{aligned}
E_1 &= (S_h^*, E_h^*, I_h^*, R_h^*, P^*, S_m^*, E_m^*, I_m^*) \\
&= (1, 0, 0, 0, \frac{(g-h)}{g}, \frac{\mu_m g + \theta_m c(g-h)}{\mu_m g}, 0, 0)
\end{aligned} \tag{6}$$

for $g - h > 0$ (which denotes the higher growth rate of plants than control rate). Even when $g = h$, there is still a DFE. In this case, the DFE becomes a DFE without invasive plants (i.e. the equilibrium E_1 becomes $E_2 = (1, 0, 0, 0, 0, 1, 0, 0)$.

The biological implication of this equilibrium, E_1, is that the DFE state in the presence of invasive plants and susceptible mosquitoes is possible for malaria to be eradicated from the local community even when the invasive plants are present in the target community.

3.3. **Reproduction Number** (R_0)**.** To calculate the effective reproduction number, we divide system (5) into appearance of infection and transfer of infection as matrix $F_i(x)$ and $V_i(x)$ respectively as follows:

$$F = \begin{pmatrix} 0 & 0 & 0 & (1-\epsilon\gamma)\beta_{hm}b \\ 0 & 0 & 0 & 0 \\ 0 & \frac{V_h g + K_p\theta_m(g-h)}{g(\xi_m+\mu_m)}(1-\epsilon\gamma)\beta_{hm}b\frac{\Lambda}{\mu_h} & 0 & 0 \\ 0 & 0 & 0 & 0 \end{pmatrix},$$

$$V = \begin{pmatrix} q_h+\mu_h & 0 & 0 & 0 \\ -q_h & \delta_h+\mu_h+v_h & 0 & 0 \\ 0 & 0 & q_m+\xi_m+\mu_m & 0 \\ 0 & 0 & -q_m & \xi_m+\mu_m \end{pmatrix}$$

$$V^{-1} = \begin{pmatrix} \frac{1}{q_h+\mu_h} & 0 & 0 & 0 \\ \frac{q_h}{(q_h+\mu_h)(v_h+\delta_h+\mu_h)} & \frac{1}{\delta_h+\mu_h+v_h} & 0 & 0 \\ 0 & 0 & \frac{1}{q_m+\xi_m+\mu_m} & 0 \\ 0 & 0 & \frac{q_m}{(\mu_m+\xi_m)(q_m+\mu_m+\xi_m)} & \frac{1}{(\mu_m+\xi_m)} \end{pmatrix}$$

Therefore, the spectral radius of FV^{-1} gives the effective reproduction number as shown below.

$$R_{01} = \sqrt{\frac{k_1k_2k_3q_m(q_m+\mu_m)}{\mu_m(q_h+\mu_h)(v_h+\delta_h+\mu_h)(q_m+\mu_m)(q_m+\mu_m)}}$$

where $k_1 = (1-\epsilon\gamma)\beta_{hm}b, k_2 = (1-\epsilon\gamma)\beta_{mh}b, k_3 = \frac{\mu_m g+\theta_m c(g-h)}{\mu g}$.

3.4. **Case II: When there are no invasive plants in human environment.** Here, we recompute the basic reproduction number of system (5), where there are no invasive plants. Equilibrium, E_2, is used in this case and is given by

$$\begin{aligned} E_2 &= (S_h^+, E_h^+, I_h^+, R_h^+, P^+, S_m^+, E_m^+, I_m^+) \\ &= (1, 0, 0, 0, 0, 1, 0, 0) \end{aligned} \tag{7}$$

3.5. **Analysis of basic reproduction number** (R_0)**.** Following the matrix generation approach, used above, we calculated the reproduction number of the homogeneous system corresponding to equilibrium, E_2 to be

$$R_{02} = \sqrt{\frac{k_1k_2q_m(q_m+\mu_m)}{\mu_m(q_h+\mu_h)(v_h+\delta_h+\mu_h)(q_m+\mu_m)(q_m+\mu_m)}}$$

where $k_1 = (1-\epsilon\gamma)\beta_{hm}b, k_2 = (1-\epsilon\gamma)\beta_{mh}b$.

3.6. **Local asymptotic stability (LAS) of E_1 equilibrium.** Linearising the spatial homogeneous model(5) with the corresponding equilibrium, E_1, we obtained the following:

$$J(E_1) = \begin{pmatrix} -\mu_h & 0 & \delta_h & \alpha_h & 0 & 0 & 0 & -k_1 \\ 0 & -m_1 & 0 & 0 & 0 & 0 & 0 & k_1 \\ 0 & q_h & -m_2 & 0 & 0 & 0 & 0 & 0 \\ 0 & 0 & v_h & -(\alpha_h+\mu_h) & 0 & 0 & 0 & 0 \\ 0 & 0 & 0 & 0 & h-g & 0 & 0 & 0 \\ 0 & 0 & -k_2k_3 & 0 & \theta_m c & -\mu_m & 0 & 0 \\ 0 & 0 & k_2k_3 & 0 & 0 & 0 & -(q_m+\mu_m) & 0 \\ 0 & 0 & 0 & 0 & 0 & 0 & q_m & -\mu_m \end{pmatrix} \tag{8}$$

where $m_1 = (q_h + \mu_h), m_2 = (\delta_h + \mu_h + v_h)$

The eigenvalues corresponding to equation (8) is given by $\lambda_1 = h - g < 0, \lambda_2 = -\mu_h, \lambda_3 = -(\alpha_h + \mu_h), \lambda_4 = -\mu_m$

The rest four roots can be obtain from the following polynomial

$$P(\lambda) = \lambda^4 + A_0\lambda^3 + A_1\lambda^2 + A_2\lambda + A_3 \tag{9}$$

where

$$\begin{aligned} A_0 &= \delta_h + 2\mu_h + q_h + v_h + 2\mu_m + q_m \\ A_1 &= \delta_h\mu_h + \mu_h^2 + 2\delta_h\mu_m + 4\mu_h\mu_m + \delta_h q_m + 2\mu_h q_m + 2q_h\mu_m \\ &\quad + v_h q_m + q_h q_m + 2v_h\mu_m + \delta_h q_h + \mu_h q_h + q_h v_h + \mu_h v_h + \mu_m^2 + \mu_m q_m \\ A_2 &= 2\delta_h\mu_h\mu_m + \delta_h\mu_m^2 + 2\mu_h^2\mu_m + 2\mu_h\mu_m^2 + \delta_h\mu_h q_m + 2\delta_h q_h\mu_m \\ &\quad + \delta_h\mu_m q_m + \delta_h q_h q_m + \mu_h^2 q_m + \mu_h q_h q_m + 2\mu_h q_h\mu_m + 2\mu_h\mu_m q_m + q_h\mu_m^2 \\ &\quad + q_h\mu_m q_m + \mu_h v_h q_m + 2q_h v_h\mu_m + v_h\mu_m q_m + q_h v_h q_m + 2\mu_h v_h\mu_m + v_h\mu_m^2 \\ A_3 &= -k_1k_2k_3q_m + \delta_h\mu_h\mu_m^2 + \mu_h^2\mu_m^2 + \delta_h\mu_h\mu_m q_m + \delta_h q_h\mu_m^2 + \delta_h q_h\mu_m q_m \\ &\quad + \mu_h^2\mu_m q_m + \mu_h q_h\mu_m^2 + \mu_h q_h\mu_m q_m + \mu_h v_h\mu_m q_m + q_h v_h\mu_m^2 + q_h v_h\mu_m q_m + \mu_h v_h\mu_m^2 \\ &= \frac{(k_0 - k_1k_2k_3q_m)[\mu_m(q_h+\mu_h)(v_h+\delta_h+\mu_h)(q_m+\mu_m)]}{k_1k_2k_3q_hq_m + (\mu(q_h+\mu_h)(v_h+\delta_h+\mu_h)(q_m+\mu_m))}\left[R_{01}^2 - 1\right] \end{aligned}$$

where

$$\begin{aligned} k_0 &= \delta_h\mu_h\mu_m^2 + \mu_h^2\mu_m^2 + \delta_h\mu_h\mu_m q_m + \delta_h q_h\mu_m^2 \\ &\quad + \delta_h q_h\mu_m q_m + \mu_h^2\mu_m q_m + \mu_h q_h\mu_m^2 + \mu_h q_h\mu_m q_m \\ &\quad + \mu_h v_h\mu_m q_m + q_h v_h\mu_m^2 + q_h v_h\mu_m q_m + \mu_h v_h\mu_m^2 \end{aligned}$$

3.7. **Remark 1.** Clearly, A_0, A_1, $A_2 > 0$ and $A_3 > 0$ provided that $R_{01}^2 < 1$ and $\frac{(k_0 - k_1k_2k_3q_m)[\mu_m(q_h+\mu_h)(v_h+\delta_h+\mu_h)(q_m+\mu_m)]}{[k_1k_2k_3q_m + (\mu(q_h+\mu_h)(v_h+\delta_h+\mu_h)(q_m+\mu_m))]} < 0$. Thus, the DFE corresponding to the continuous presence of invasive plants in human environment is locally asymptotically stable (LAS).

3.8. **Local asymptotic stability (LAS) of E_2 equilibrium.** Also, we linearised the homogeneous part of our model equations (5) with the corresponding equilibrium, E_2 and

obtained the following:

$$J(E_2) = \begin{pmatrix} -\mu_h & 0 & \delta_h & \alpha_h & 0 & 0 & 0 & -k_1 \\ 0 & -m_1 & 0 & 0 & 0 & 0 & 0 & k_1 \\ 0 & q_h & -m_2 & 0 & 0 & 0 & 0 & 0 \\ 0 & 0 & v_h & -(\alpha_h+\mu_h) & 0 & 0 & 0 & 0 \\ 0 & 0 & 0 & 0 & g-h & 0 & 0 & 0 \\ 0 & 0 & -k_2 & 0 & \theta_m c & -\mu_m & 0 & 0 \\ 0 & 0 & k_2 & 0 & 0 & 0 & -(q_m+\mu_m) & 0 \\ 0 & 0 & 0 & 0 & 0 & 0 & q_m & -\mu_m \end{pmatrix} \tag{10}$$

where $m_1 = (q_h + \mu_h), m_2 = (\delta_h + \mu_h + v_h)$ The eigenvalues corresponding to equation (10) is given by $x_1 = g - h = 0, x_2 = -\mu_h, x_3 = -(\alpha_h + \mu_h), x_4 = -\mu_m$

The rest four roots can be obtain from the following polynomial

$$x^4 + B_0x^3 + B_1x^2 + B_2x + B_3 = 0 \tag{11}$$

where

$$\begin{aligned} B_0 &= \delta_h + 2\mu_h + q_h + v_h + 2\mu_m + q_m \\ B_1 &= \delta_h\mu_h + \mu_h^2 + 2\delta_h\mu_m + 4\mu_h\mu_m + \delta_h q_m + 2\mu_h q_m + 2q_h\mu_m \\ &\quad + v_h q_m + q_h q_m + 2v_h\mu_m + \delta_h q_h + \mu_h q_h + q_h v_h + \mu_h v_h + \mu_m^2 + \mu_m q_m \\ B_2 &= 2\delta_h\mu_h\mu_m + \delta_h\mu_m^2 + 2\mu_h^2\mu_m + 2\mu_h\mu_m^2 + \delta_h\mu_h q_m + 2\delta_h q_h\mu_m \\ &\quad + \delta_h\mu_m q_m + \delta_h q_h q_m + \mu_h^2 q_m + \mu_h q_h q_m + 2\mu_h q_h\mu_m + 2\mu_h\mu_m q_m + q_h\mu_m^2 \\ &\quad + q_h\mu_m q_m + \mu_h v_h q_m + 2q_h v_h\mu_m + v_h\mu_m q_m + q_h v_h q_m + 2\mu_h v_h\mu_m + v_h\mu_m^2 \\ B_3 &= -k_1k_2q_m + \delta_h\mu_h\mu_m^2 + \mu_h^2\mu_m^2 + \delta_h\mu_h\mu_m q_m + \delta_h q_h\mu_m^2 + \delta_h q_h\mu_m q_m \\ &\quad + \mu_h^2\mu_m q_m + \mu_h q_h\mu_m^2 + \mu_h q_h\mu_m q_m + \mu_h v_h\mu_m q_m + q_h v_h\mu_m^2 + q_h v_h\mu_m q_m + \mu_h v_h\mu_m^2 \\ &= \frac{(k_0 - k_1k_2q_m)[\mu_m(q_h+\mu_h)(v_h+\delta_h+\mu_h)(q_m+\mu_m)]}{k_1k_2q_m + (\mu(q_h+\mu_h)(v_h+\delta_h+\mu_h)(q_m+\mu_m))} \left[R_{02}^2 - 1\right] \end{aligned}$$

where

$$\begin{aligned} k_0 &= \delta_h\mu_h\mu_m^2 + \mu_h^2\mu_m^2 + \delta_h\mu_h\mu_m q_m + \delta_h q_h\mu_m^2 \\ &\quad + \delta_h q_h\mu_m q_m + \mu_h^2\mu_m q_m + \mu_h q_h\mu_m^2 + \mu_h q_h\mu_m q_m \\ &\quad + \mu_h v_h\mu_m q_m + q_h v_h\mu_m^2 + q_h v_h\mu_m q_m + \mu_h v_h\mu_m^2 \end{aligned}$$

3.9. **Remark 1.** Clearly, B_0, B_1, $B_2 > 0$ and $B_3 > 0$ provided that $R_{02}^2 < 1$ and $\frac{(k_0 - k_1k_2q_hq_m)[\mu_m(q_h+\mu_h)(v_h+\delta_h+\mu_h)(q_m+\mu_m)]}{[k_1k_2q_m+(\mu(q_h+\mu_h)(v_h+\delta_h+\mu_h)(q_m+\mu_m))]} < 0$. Since one of the eigenvalues is zero, further analysis using the Center Manifold Theory, will have to be used in establishing the LAS of E_2 in the manifold of interest. However, since the other eigenvalues are negative, with the associated reproduction number less than unity, we conjecture that E_2, at most stable, and an attractor of trajectories in its neighbourhood. E_2 is stable but may not be asymptotically stable, since this DFE exists only when $g = h$.

These results shows an important effect of the presence of invasive plants on malaria dynamics: they can lead to the existence of two DFEs, an important contribution to knowledge.

3.10. **Disease endemic equilibrium (DEE).** To obtain this equilibrium, we set the right hand sides of (5), and solve for the state variables. After several calculations, we have that

$$E_3 = (S_h^{**}, E_h^{**}, I_h^{**}, R_h^{**}, P^{**}, S_m^{**}, E_m^{**}, I_m^{**})$$

where,

$$\begin{aligned}
S_h^{**} &= \frac{\mu_h a_1 a_2 a_3}{(a_1 a_2 a_3 - \delta_h \alpha_h - \delta_h \mu_h - \alpha_h v_h)\lambda_h^{**} + \mu_h a_1 a_2 a_3} \\
E_h^{**} &= \frac{a_2 a_3 \mu_h \lambda_h^{**}}{(a_1 a_2 a_3 - \delta_h \alpha_h - \delta_h \mu_h - \alpha_h v_h)\lambda_h^{**} + \mu_h a_1 a_2 a_3} \\
I_h^{**} &= \frac{\mu_h a_3 q_h \lambda_h^{**}}{(a_1 a_2 a_3 - \delta_h \alpha_h - \delta_h \mu_h - \alpha_h v_h)\lambda_h^{**} + \mu_h a_1 a_2 a_3} \\
R_h^{**} &= \frac{\mu_h v_h q_h \lambda_h^{**}}{(a_1 a_2 a_3 - \delta_h \alpha_h - \delta_h \mu_h - \alpha_h v_h)\lambda_h^{**} + \mu_h a_1 a_2 a_3} \\
P^{**} &= \frac{K_p(g-h)}{g}, g > h \\
S_m^{**} &= \frac{\mu_m g + \theta_m c(g-h)}{g(\mu_m + \lambda_m^{**})}, \\
E_m^{**} &= \frac{\lambda_m^{**}(\mu_m g + \theta_m c(g-h))}{g(\mu_m + \lambda_m^{**})(q_m + \mu_m)}, \\
I_m^{**} &= \frac{\lambda_m^{**}(\mu_m g + \theta_m c(g-h)}{\mu_m g(\mu_m + \lambda_m^{**})(q_m + \mu_m)}, \\
N_h^{**} &= \frac{\mu_h(a_1 a_2 a_3 + \lambda_h^{**}(a_2 a_3 + a_3 q_h + v_h q_h))}{(a_1 a_2 a_3 - \delta_h \alpha_h - \delta_h \mu_h - \alpha_h v_h)\lambda_h^{**} + \mu_h a_1 a_2 a_3}
\end{aligned}$$

where

$$a_1 = q_h + \mu_h, a_2 = \delta_h + \mu_h + v_h, a_3 = \mu_h + \alpha_h$$

and

$$\lambda_h^{**} = \phi \beta_{hm} \frac{b I_m^{**}}{N_h^{**}}, \lambda_m^{**} = \phi \beta_{mh} \frac{b I_h^{**}}{N_h^{**}}$$

where

$$\phi = (1 - \epsilon\gamma)$$

3.11. **Backward bifurcation phenomenon.** Backward bifurcation may occur under certain conditions for $R_{01}^2 < 1$. The presence of backward bifurcation indicates that the necessary requirement of $R_{01}^2 < 1$, is not sufficient for disease elimination. The Center Manifold Theory will be used to prove the conditions on existence of backward bifurcation. To investigate the existence of the backward bifurcation of the spatially homogeneous of Eq. (5), we shall rewrite it in vector form as:

$$\frac{dY}{dt} = H(y)$$

where

$$X = (y_1, y_2, y_3, y_4, y_5, y_6, y_7, y_8)^T$$

and

$$H = (h_1, h_2, h_3, h_4, h_5, h_6, h_7, h_8)^T$$

so that

$$S_h = y_1, E_h = y_2, I_h = y_3, R_h = y_4, P = y_5, S_m = y_6, E_m = y_7, I_m = y_8$$

.
Thus, it becomes

$$\begin{aligned}
\dot{y_1} &= h_1 = \mu_h(1-y_1) + \delta_h y_3 + \alpha_h y_4 - (1-\epsilon\gamma)\beta_{hm} b y_1 y_8 \\
\dot{y_2} &= h_2 = (1-\epsilon\gamma)\beta_{hm} b y_1 y_8 - (q_h + \mu_h) y_2 \\
\dot{y_3} &= h_3 = q_h y_2 - (\delta_h + \mu_h + v_h) y_3 \\
\dot{y_4} &= h_4 = v_h y_3 - (\mu_h + \alpha_h) y_4 \\
\dot{y_5} &= h_5 = g(1-y_5) y_5 - h y_5 \\
\dot{y_6} &= h_6 = \mu_m(1-y_6) + \theta_m c y_5 - (1-\epsilon\gamma) b x y_3 y_6 \\
\dot{y_7} &= h_7 = (1-\epsilon\gamma) b x y_3 y_6 - (q_m + \mu_m) y_7 \\
\dot{y_8} &= h_8 = q_m y_7 - \mu_m y_8
\end{aligned}$$

Choosing β_{mh} as the bifurcation parameter at $R_{01} = 1$, We have

$$\beta_{mh} = \beta^*_{mh} = \sqrt{\frac{k_1 k_2 k_3 q_m(q_m + \mu_m)}{\mu_m(q_h + \mu_h)(v_h + \delta_h + \mu_h)(q_m + \mu_m)(q_m + \mu_m)}}$$

By virtue of the Center Manifold Theory (Castillo Chavez and Song, 2014), we calculated the bifurcation parameter to be

$$\begin{aligned}
a = v_1 \sum_{i,j=1}^{8} w_i w_j \frac{\partial^2 h_1}{\partial y_i \partial y_j} + v_2 \sum_{i,j=1}^{8} w_i w_j \frac{\partial^2 h_2}{\partial y_i \partial y_j} \\
+ v_5 \sum_{i,j=1}^{8} w_i w_j \frac{\partial^2 h_5}{\partial y_i \partial y_j} + v_6 \sum_{i=1}^{8} w_i w_j \frac{\partial^2 h_6}{\partial y_i \partial y_j} \\
+ v_7 \sum_{i,j=1}^{8} w_i w_j \frac{\partial^2 h_7}{\partial y_i \partial y_j} \\
= (1-\epsilon\gamma)\beta^*_{hm} b v_2 + (1-\epsilon\gamma)\beta^*_{mh} b v_7 > 0.
\end{aligned}$$

Also,

$$\begin{aligned}
b = v_1 \sum_{i=1}^{8} w_i \frac{\partial^2 h_1}{\partial y_i \partial \beta^*_{hm}} + v_2 \sum_{i=1}^{8} w_i \frac{\partial^2 h_2}{\partial y_i \partial \beta^*_{hm}} \\
+ v_6 \sum_{i=1}^{8} w_i \frac{\partial^2 h_6}{\partial y_i \partial \beta^*_{mh}} + v_7 \sum_{i=1}^{8} w_i \frac{\partial^2 h_7}{\partial y_i \partial \beta^*_{mh}} \\
= (1-\epsilon\gamma) b v_2 + \frac{(1-\epsilon\gamma) b(\mu_m g + \theta_m c(g-h)) v_7}{\mu_m g} > 0.
\end{aligned}$$

We therefore conclude that a backward bifurcation occurs since $a > 0$ and $b > 0$.

4. Numerical simulations

Here, we use Runge-kutta method to simulate the ordinary differential equations part of the model while a constructed finite difference scheme was used to simulate the partial differential equations part of the formulated model. In Table 3, we present the numerical values of the model equations' parameters as shown below.

$$D = \frac{L^2}{2T}$$

where L is the average distance covered by mosquito in a day and T is the time taken to travel [24].

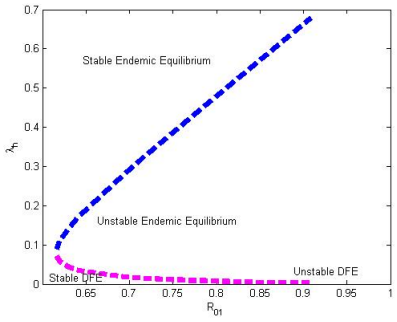

FIGURE 2. Bifurcation diagram of the homogeneous part of Equations (3)

4.1. **PDE Simulation of Equations (4).** In this section, we carefully simulate the PDE part of the formulated model in order to explore the behaviour of the vector and the disease transmission dynamics.

$$E_m(x,0) = I_m(x,0) = \begin{cases} \frac{1}{N_m}, & |x| \leq L; \\ 0, & |x| > L. \end{cases}$$

$$E_h(x,0) = I_h(x,0) = R_h(x,0) = 0$$

Parameter	Value	Baseline	Reference
μ_h	0.00004643/day	$(\frac{1}{61\times365} - \frac{1}{58\times365})$/day	Kenya National Bureau of Statistics
β_{hm}	0.24/day	(0.072 - 0.64)/day	[30]
β_{mh}	0.14/day	(0.027 - 0.64)/day	[30]
q_h	0.083/day	(0.06 - 0.203)/day	[30])
α_h	0.000017/day	(0.0000055 - 0.011)/day	[32]
v_h	0.00265/day	(0.001 - 0.023)/day	[30]
K_p	1	$(0-1)$	Variable
ϵ	0.5	(0 - 1)	Variable
γ	0.6	(0 - 1)	Variable
δ_h	0.0003454/day	(0.0000000001 - 0.00041)/day	[32]
b	0.5	(0 - 1)	Variable
θ_m	0.343/day	(0.333 - 1)/day	[30]
q_m	0.091	(0.029 - 0.33)/day	[32]
g	1.84	(1 - 500)/day	[30]
μ_m	0.1041	(0.0941 - 0.1234)/day	[32]
h	0.05	(0.01 - 0.1)/day	Variable
D	$3.125km^2$	($2.5km^2$ - $12km^2$)/day	Computed
k	4.5	(0km - 6km)/day	[25]
L	2.5	(3km - 5km)/day	[25]

TABLE 2. Description of the model parameters' values

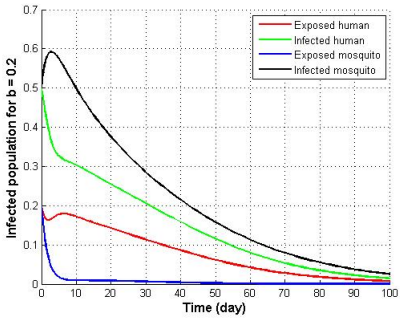

FIGURE 3. Plot of the infected population over time

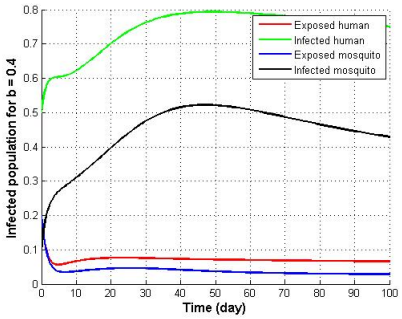

FIGURE 4. Plot of the infected population over time

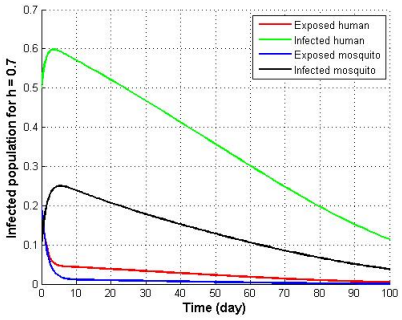

FIGURE 5. Plot of the infected population over time

5. TRAVELLING WAVE ANALYSIS OF THE SPATIAL SYSTEM

In this section, we shall assess the spatial spread of malaria disease with spatial dispersion of vectors. Using our formulated model, we obtain the traveling wave system of

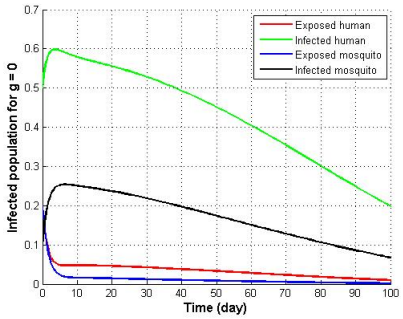

FIGURE 6. Plot of the infected population over time

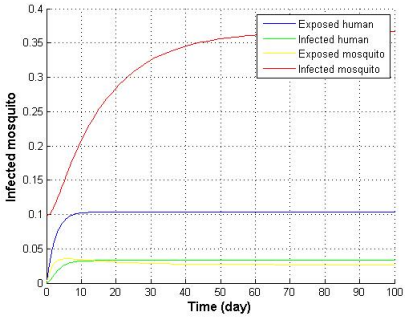

FIGURE 7. Plot of the infected compartment of Equations (4) with initial conditions $e_h(0) = 0, i_h(0) = 0, e_m(0) = 0$ and $i_m(0) = 0.1$

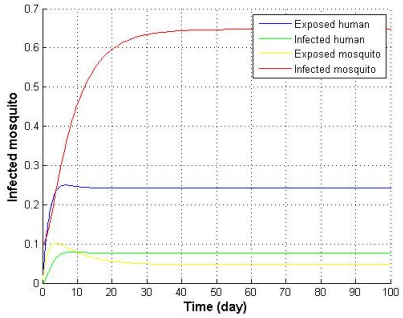

FIGURE 8. Plot of the infected compartment of Equations (4) with initial conditions $e_h(0) = 0, i_h(0) = 0, e_m(0) = 0$ and $i_m(0) = 0.3$

equations to be

$$\begin{aligned}
e\prime + \frac{c_1}{v}(1 - e_h - i_h - r_h)i_m - \frac{(q_h + \mu_h)}{v}e_h = 0 \\
i\prime_h + \frac{q_h}{v}eh - \frac{(\delta_h + \mu_h + v_h)}{v}i_h = 0 \\
r\prime_h + \frac{v_h}{v}i_h - \frac{(\mu_h + \alpha_h)}{v}r_h = 0 \\
De_m\prime\prime - (k - v)e\prime_m - \frac{c_2}{v}(1 - e_m - i_m)i_h + (q_m + \mu_m)e_m = 0 \\
Di_m\prime\prime - (k - v)i\prime_m - q_m e_m - \mu_m i_m = 0
\end{aligned} \tag{12}$$

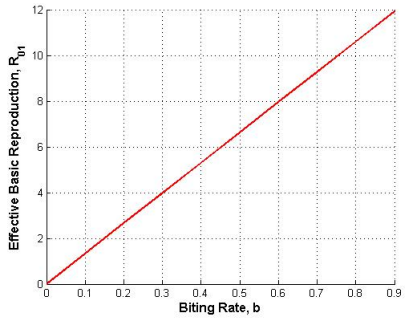

FIGURE 9. Plot of the effective reproduction number, R_{01} over the biting rate, b

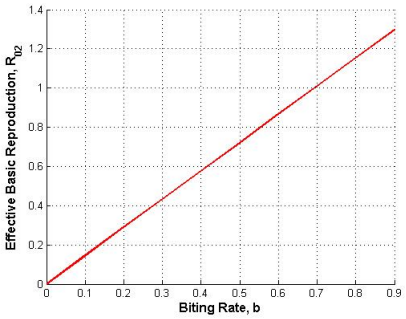

FIGURE 10. Plot of the effective reproduction number, R_{02} over the biting rate, b

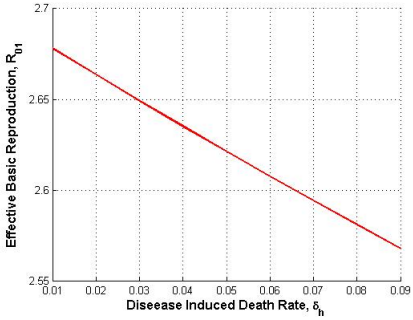

FIGURE 11. Plot of the effective reproduction number, R_{01} over the disease induced death rate, δ_h

where $c_1 = \phi\beta_{hm}b, c_2 = \phi\beta_{mh}b$ and $\phi = 1 - \epsilon\gamma$.

This system is equivalent to the following system of first-order differential equations:

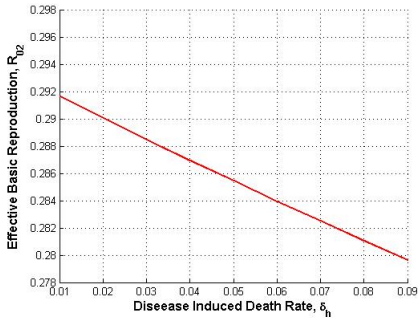

FIGURE 12. Plot of the effective reproduction number, R_{02} over the disease induced death rate, δ_h

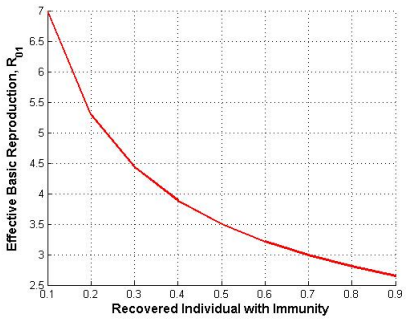

FIGURE 13. Plot of the effective reproduction number, R_{01} over the recovered individuals with immunity, v_h

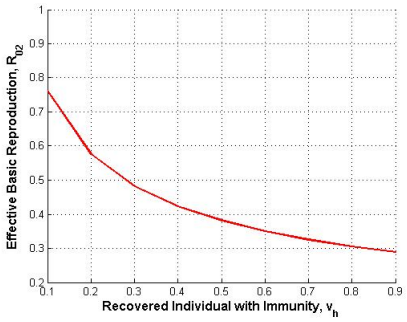

FIGURE 14. Plot of the effective reproduction number, R_{02} over the recovered individuals with immunity, v_h

$$
\begin{aligned}
\frac{de_h}{dz} &= -\frac{c_1}{v}(1-e_h-i_h-r_h)i_m + \frac{(q_h+\mu_h)}{v}e_h + \frac{\delta_h+v_h+\mu_h}{v}i_h \\
\frac{di_h}{dz} &= -\frac{q_h}{v}e_h + \frac{(\delta_h+v_h+\mu_h)}{v}i_h \\
\frac{r_h}{dz} &= \frac{v_h}{v}i_h + \frac{(\alpha_h+\mu_h)}{v}r_h \\
\frac{e_m}{dz} &= u_1 \\
\frac{du_1}{dz} &= \frac{1}{D}(k-v)u_1 - \frac{c_2(1-e_m-i_m)}{D}i_h + \frac{(q_m+\mu_m)}{D}e_m \\
\frac{di_m}{dz} &= u_2 \\
\frac{du_2}{} &= \frac{1}{}
\end{aligned}
\tag{13}
$$

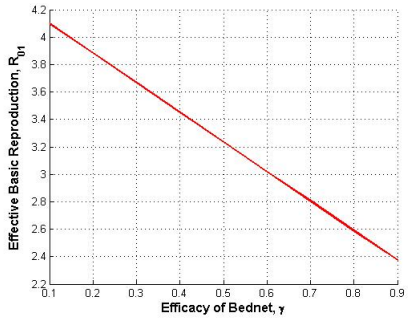

FIGURE 15. Plot of the effective reproductive number, R_{01} over the bed net efficacy, γ

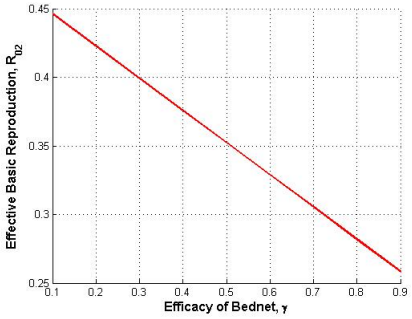

FIGURE 16. Plot of the effective reproductive number, R_{02} over the bed net efficacy, γ

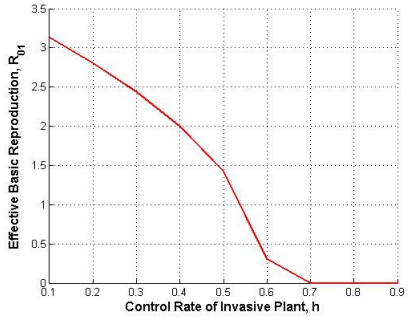

FIGURE 17. Plot of the effective reproductive number, R_{01} over the invasive plants control rate, h

where

$$\frac{di_m}{dt} = i_m^{''}(z), \frac{de_m}{dt} = e_m^{''}(z)$$

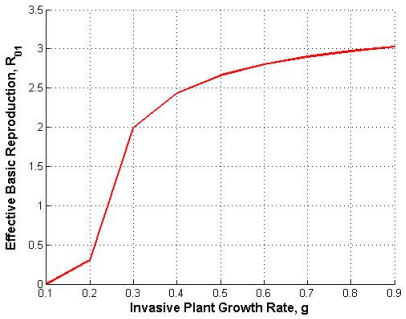

FIGURE 18. Plot of the effective reproductive number, R_{01} over the invasive plants growth rate, g

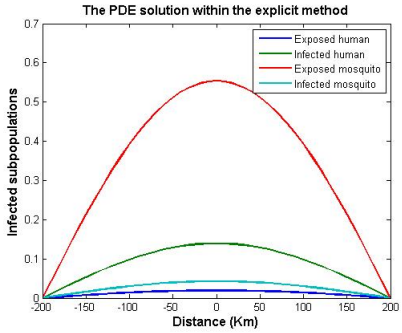

FIGURE 19. Graph of the solutions of system (4) for the paramters outlined in Table 2, considering the diffusion coefficient $D = 3.125km^2$/day and the advection coefficient $k = 0$.

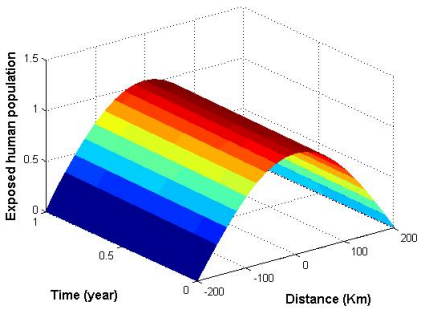

FIGURE 20. 3D plot of exposed human population

The corresponding eigenvalues of the wave equations are the roots of the polynomial

$$m(\Psi) = \Psi^7 + b_0\Psi^6 + b_1\Psi^5 + b_2\Psi^4 + b_3\Psi^3 + b_4\Psi^2 + b_5\Psi + b_6 \tag{14}$$

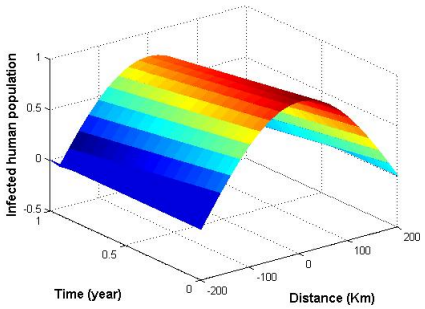

FIGURE 21. 3D plot of infected human population

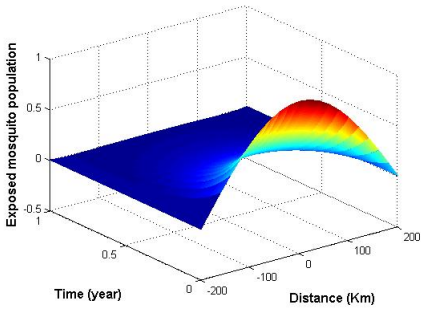

FIGURE 22. 3D plot of exposed mosquito population

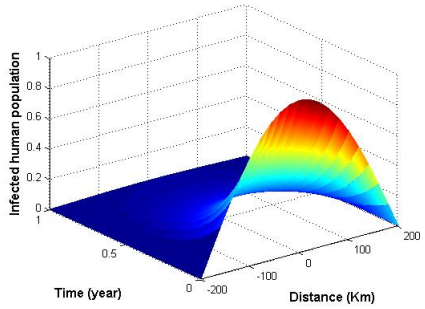

FIGURE 23. 3D plot of infected mosquito population

where

$b0 = P1 + P2 + P3 + P5 + P6$

$b_1 = -(\frac{\mu_m}{D} - P_1P_2 - P_3P_2 - P_5P_2 - P_6P_2 - P_1P_3 + P_4 - P_1P_5 - P_3P_5 - P_1P_6 - P_3P_6 - P_5P_6)$

$b_2 = -(\frac{P_3\mu_m}{D} - \frac{P_1\mu_m}{D} - \frac{P_2\mu_m}{D} - \frac{P_5\mu_m}{D} + P_1P_2P_3 - P_4P_3 + P_1P_5P_3 + P_2P_5P_3 + P_1P_6P_3 +$

$P_2P_6P_3 + P_5P_6P_3 - P_1P_4 - P_2P_4 + P_1P_2P_5 + P_1P_2P_6 - P_4P_6 + P_1P_5P_6 + P_2P_5P_6)$

$b_3 = -(-\frac{P_4\mu_m}{D} + \frac{P_1P_2\mu_m}{D} + \frac{P_1P_3\mu_m}{D} + \frac{P_2P_3\mu_m}{D} + \frac{P_1P_5\mu_m}{D} + \frac{P_2P_5\mu_m}{D} + \frac{P_3P_5\mu_m}{D} + P_1P_2P_4 + P_1P_3P_4 + P_2P_3P_4 + P_1P_6P_4 + P_2P_6P_4 + P_3P_6P_4 - P_1P_2P_3P_5 - P_1P_2P_3P_6 - P_1P_2P_5P_6 - P_1P_3P_5P_6 - P_2P_3P_5P_6)$

$b_4 = -(\frac{P_1P_4\mu_m}{D} + \frac{P_2P_4\mu_m}{D} + \frac{P_3P_4\mu_m}{D} - \frac{P_1P_2P_3\mu_m}{D} - \frac{P_1P_2P_5\mu_m}{D} - \frac{P_1P_3P_5\mu_m}{D} - \frac{P_2P_3P_5\mu_m}{D} - P_1P_2P_3P_4 - P_1P_2P_6P_4 - P_1P_3P_6P_4 - P_2P_3P_6P_4 + P_1P_2P_3P_5P_6)$

$b_5 = -(\frac{c_1c_2q_hq_m}{D^2v^2} + \frac{P_1P_2P_3P_5\mu_m}{D} - \frac{P_1P_2P_4\mu_m}{D} - \frac{P_1P_3P_4\mu_m}{D} - \frac{P_2P_3P_4\mu_m}{D} + P_1P_2P_3P_4P_6)$

$b_6 = \frac{c_1c_2P_3q_hq_m}{D^2v^2} - \frac{P_1P_2P_3P_4\mu_m}{D}$

and $P_1 = \frac{q_h+\mu_h}{v}, P_2 = \frac{\delta_h+v_h+\mu_h}{v}, P_3 = \frac{\alpha_h+\mu_h}{v}, P_4 = \frac{q_m+\mu_m}{D}, P_5 = P_6 = \frac{k-v}{D}$

5.1. **Numerical simulation of wave equation.** Here, we carried out the numerical simulations of the wave equation to investigating the results obtained from the PDE simulations studied above.

Ψ	$v = 0.001(k = 0)$	$v = 0.001(k = 4.5)$
Ψ_1	$-0.201146 - 0.11614i$	$-0.144577 - 0.0834711i$
Ψ_2	$-0.201146 + 0.11614i$	$-0.144577 + 0.0834711i$
Ψ_3	$0.000020719 - 0.232251i$	$-0.0000004429 - 0.166943i$
Ψ_4	$0.000020719 + 0.232251i$	$-0.0000004429 + 0.166943i$
Ψ_5	$0.201125 - 0.1161081i$	$0.144577 - 0.0834718i$
Ψ_6	$0.201125 + 0.1161081i$	$0.144577 + 0.0834718i$
Ψ_7	1440	10440

TABLE 3. Different velocity values with their respective roots of a polynomial (14) D = 3.125 km^2

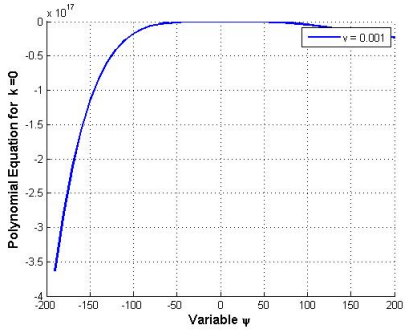

FIGURE 24. Graph of the polynomial $m(\psi)$ for the parameters outlined in Table 3

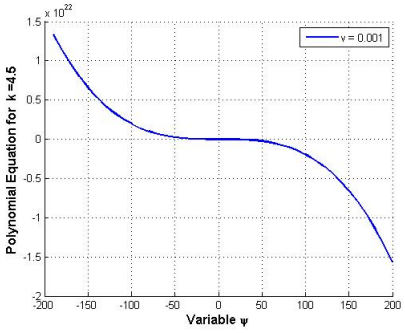

FIGURE 25. Graph of the polynomial $m(\psi)$ for the parameters outlined in Table 3

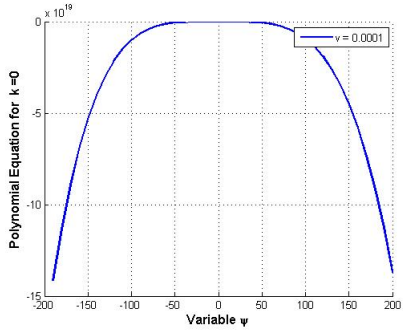

FIGURE 26. Graph of the polynomial $m(\psi)$ for the parameters outlined in Table 3

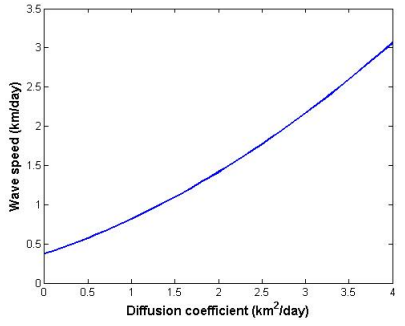

FIGURE 27. Graph of the propagation speed as a function of the diffusion coefficient D when $k = 0$. The values used for the other parameters are outlined in Table 3

6. DISCUSSION

Figure 2 shows the backward bifurcation diagram of the homogeneous part of Equation (3). The system is stable at $R_{01} < 1$ and unstable if otherwise. Figure 3 shows the plots of infected sub-populations over time when $b = 0.2$, the exposed mosquito population declined to a steady state after a short time while the rest of the sub-populations declined to a steady state after a long period of time. Figure 4 is a repetition of Figure 3 by increasing the biting rate to $b = 0.4$. This shows that even at a slight change of biting rate, the disease can trigger and persists. Figure 5 is a repetition of Figure 4 with control rate of invasive plants, $h = 0.7$, both the infected human and mosquito sub-populations approached zero steady state overtime. Figure 6 is a repetition of Figure 4 with growth rate of invasive plants, $g = 0$, both the infected human and mosquito attained a steady state faster. Figure 7 shows the plots of the infected sub-populations of Equations (4) with the initial values $e_h = i_h = e_m = 0$ and $i_m = 0.1$. Each of the sub-populations grows beyond its initial value due to the presence of parasite infection in the population. Figure 8 is a repetition of Figure 7 with $i_m = 0.3$. Each of the sub-populations grow higher than the growth observed in Figure 7 due to 20% increase of the infected mosquito sub-population.

Figure 9 shows a linear relationship between the effective basic reproduction number, R_{01} and the biting rate parameter, b. it can be observed that a high biting rate leads to malaria endemicity in human population. Figure 10 shows a linear relationship between the effective basic reproduction number, R_{02} and the biting rate parameter, b. it can be observe that a high biting rate led to malaria endemicity in human population. Figure 11 shows a linear relationship between the effective basic reproduction number, R_{01} and the biting rate parameter, δ_h. The disease induced death rate δ_h of human population shows a drastic reduction of malaria disease. Figure 12 shows a linear relationship between the effective basic reproduction number, R_{02} and the biting rate parameter, δ_h. The disease induced death rate δ_h of human population shows a drastic reduction of malaria disease. Figure 13 shows a linear relationship between the effective basic reproduction number, R_{01} and the biting rate parameter, v_h. The recovered rate, v_h parameter has high impact on malaria disease reduction. Figure 14 shows a linear relationship between the effective basic reproduction number, R_{02} and the biting rate parameter, v_h. The recovered rate, v_h parameter has high impact on malaria disease reduction. Figure 15 shows a linear relationship between the effective basic reproduction number, R_{01} and the biting rate parameter, γ. The Efficacy of bednet, γ parameter also has high impact on malaria disease control. Figure 16 shows a linear relationship between the effective basic reproduction number, R_{02} and the biting rate parameter, γ. The Efficacy of bednet, γ parameter also has high impact on malaria disease control. Figure 17 shows a relationship plot between the effective basic reproduction number, R_{01} and the control of invasive plant parameter h, The malaria disease will be eliminated totally if 70% of the invasive plants can be achieved based on the parameter values of this model. Figure 18 shows a relationship between the R_{01} and the growth rate parameter, g. The malaria disease burden persists higher with increase of invasive plants.

Figure 19 shows the minimum speed of the disease transmission. The disease spread faster with increase of diffusion and advection coefficients of the model. Figure 20 shows the minimum speed of the disease transmission. The exposed human sub-population grows faster with increase of diffusion and advection coefficients of the model. Figure 21 shows the minimum speed of the disease transmission. The infected human sub-population grows faster with increase of diffusion and advection coefficients of the model. Figure 22 shows the minimum speed of the disease transmission. The exposed mosquito sub-population

grows faster with increase of diffusion and advection coefficients of the model. Figure 23 shows the minimum speed of the disease transmission. The infected mosquito subpopulation grows faster with increase of diffusion and advection coefficients of the model. There is a presence of backward bifurcation phenomenon of the model even when control measure ensures that the reproduction number is less than one, there is still a possibility of disease presence in the community.

If 70% of invasive plants can be control, the disease can be eliminated based on the parameter values of this model. Even with invasive plants , we can control malaria. Those plants have their usefulness ecologically. Efficacy of bed net and treatment of infected individual reduce malaria burden in human population. The higher the diffusion, D value the higher the distribution of the malaria disease in human population.

Figure 24 shows a plot of polynomial equation at $k = 0$ over its eigenvalues. The wave speed increases with the negative eigenvalues and decreases with the positive eigenvalues. Figure 25 shows a plot of polynomial equation at $k = 4.5$ over its eigenvalues. The wave speed decreases as the eigenvalues of the polynomial increases. Figure 26 shows a plot of polynomial equation at $v = 0.0001$ over its eigenvalues. The wave speed increases with the negative eigenvalues and decreases with the positive eigenvalues. Figure 27 shows a relationship between the wave speed and the Diffusion coefficient. The wave speed increases as the diffusion coefficient increases and thereby leading to decrease in the disease transmission.

When we consider the advection movement (k =4.5) from the expression of the polynomial (14) coefficients $b_0, b_1, b_2, b_3, b_4, b_5$ and b_6, we observed that k appears adding the value of v. Hence, advection increases the wave speed when it is in the same direction of the wave front and decreases when it is in the opposite direction. The higher the advection coefficient is, the higher the speed of the spread of the disease, which follows a linear relationship. The flight distance rate of anopheles mosquitoes is motivated by the diffusion coefficient, D and thereby lead to more mosquitoes in human environment even if the invasive plants are located 100km a way from villages or communities.

7. CONCLUSION

This study aimed to analyze the spread of spatial dispersal dynamics of malaria disease by mathematical modeling. We propose a spatial nonlinear mathematical model that describes the impact of invasive plants and dispersion of vectors on the dynamics of malaria disease.

We analyzed the homogeneous part of the spatial model for the spread of the disease, and we found out that the model has three disease equilibria which include two DFEs and one DEE. The two DFEs occurred due to the impact of invasive plants on malaria dynamics, and this result is an important contribution to knowledge since no malaria model has this report. The stability of the equilibria were also investigated. The analysis of the possibility of the disease existence of backward bifurcation was carefully investigated. We have also formulated the traveling wave equations that enable us to determine the propagation speed of the disease transmission.

The numerical simulation of the model equations were carried out in order to validate the obtained qualitative results. We found that the effective reproduction number determines the endemic steady-state existence, the stability of the spatial dynamics and the wave speed of disease spread. This finding has biological aspects, such as the prevalence of the disease, eradication and spatial dissemination.

The results obtained for the sensitivity of the effective reproduction number showed that it is quite sensitive in relation to biting rate, disease induced death rate, recovered rate of individual with immunity, bed net efficacy, invasive plants control rate and the growth rate. Therefore, important activities for the disease control include: control of invasive plants and the provision of bed net with 70 - 90% efficacy.

Our next step was to study the spread of the disease in a human population using a spatial model and considering the same temporal dynamics. We conducted the analysis of the model under the condition $R_{01} > 1$. When this condition held, infection was established in the population, and there was a trajectory linking the disease-free equilibrium and the endemic equilibrium, enabling the determination of the minimum disease spread rate. The wave propagation speed was determined in relation to the diffusion and advection term. We also used different diffusion and advection coefficient values to assess the wave speed and to analyze the relationship between these parameters.

Finally, understanding the invasion speed could be used to support control interventions aiming to decrease the speed of propagation, even if the eradication of vectors is not possible.

Acknowledgements. The authors wish to acknowledge anonymous reviewers.

REFERENCES

[1] K.O. Achema, D. Okuonghae, and C.J. Alhassan, A Mathematical Model for Assessing the Impact of Dual-level Toxicity on Aquatic Biospecies and its Optimal Control Analysis, Mathematical Modelling and Control, AIMS, 2022, 2(3), 100-121.

[2] S. O. Adoka , D. N. Anyona, G. Dida, C. K. Kanangire, A. S. Matano, D. A. Othero, Spatial distribution and habitat characterization of mosquito species in the lake and land habitats of Western Kenya, East African Medical Journal, 93(2015) 117-126.

[3] P. M. Alarcón-Elbal, F. Collantes, S. Delacour, J. A. Delgado, R. Eritja, J. Lucientes, M. Á. Miranda, R. Molina, I. Ruiz-Arrondo, A. Sorio, B. M. Torrell, Review of ten years presence of Aedes albopictus in Spain 2004-2014: known distribution and public health concerns, *Parasit. Vectors,* 8(2015), 655. https://doi.org/10.1186/S13071-015-1262-Y.

[4] C.J. Alhassan, K.O. Achema, Modelling the Transmission Dynamics of an Avian Influenza: Qualitative and Quantitative Analysis, IOSR Journal of Mathematics, 2020, 16(3), 44-55.

[5] R. M. Anderson, R. M. May, Infectious diseases of humans: dynamics and control, Oxford University Press London, 1991, 112-200.

[6] A. B. Anna, F. M. V. Piet, Flight distance of mosquitoes (Culicdae): A metadata analysis to support the management of barrier zones around rewetted and newly constructed wetlands, *Limnologica*, 45(2014) 69-79.

[7] C. Aranda, R. Eritja, D. Roiz, First record and establishment of the mosquito Aedes albopictus in Spain, Med. Vet. Entomol. 20(2006)150-152. https://doi.org/10.1111/J.1365- 2915.2006.00605.X.

[8] J. L. Aron, R. M. May, The population dynamics of malaria, In Population Dynamics of Infectious Disease, *Chapman and Hall,* (1982) 139-179.

[9] J. L. Aron, Mathematical modeling of immunity to malaria, *Math Bios.*, 90 (1988) 385-396, doi: 10.1016/0025-5564(88)90076-4

[10] G. Bailey, C. B. Beard, N. A. Drexler, M. Fischer, C. J. Gregory, A. F. Hinckley, G. J. Kersh, N. P. Lindsey, P. S. Mead, S. K. Partridge, L. R. Petersen, G. Paz, R. Rosenberg, S. N. Visser, S. H. Waterman, Vital signs: trends in reported vectorborne disease cases - United States and territories, 2004-2016, *Morb. Mortal. Wkly Rep.* 67(2018) 496.

[11] C. M. Barker, O. J. Brady, R. G. Carvalho, G. E. Coelho, K. A. Duda, I. RElyazar, S. I. Hay, G. Hendrickx, N. Golding, M. U. G. Kraemer, A. Q. N. Mylne, F. Schaffner, F. M. Shearer, M. E. Sinka, J. P. Messina, C. G. Moore, D. M. Pigott, H. J. Teng, T. W. Scott, D. L. Smith, B. W. Van, G. R. William, The global distribution of the arbovirus vectors Aedes aegypti and Ae. Albopictus, Elife 4 (2015), e08347. https://doi.org/10.7554/ELIFE.08347.

[12] H. Barré-Cardi, G. Besnard, R. Foussadier, D. Fontenille, G. Lacour, L. Léger, G. L'Ambert, B. Roche, F. Simard, The spread of Aedes albopictus in metropolitan France: contribution of environmental drivers and human activities and predictions for a near future, *PLoS One 10*, (2015)

[13] J. C. Beier, J. Carson, S. Kahindi, J. Keating, C. M. Mbogo, Ecological limitations on aquatic mosquito predator colonization in the urban environment, *Journal of Vector Ecology,* 29(2019)3-39.

[14] M. Bonizzoni, X. Chen, G. Gasperi, A. A. James, The invasive mosquito species Aedes albopictus: current knowledge and future perspectives, *Trends Parasitology*, 29(2013) 460-468. https://doi.org/10.1016/J.PT.2013.07.003

[15] R. Charrel, X. de Lamballerie, E. Gould, S. Higgs, J. Pettersson, Emerging arboviruses: why today? One Health, 4(2017) 1-13. https://doi.org/10.1016/J.ONEHLT.2017.06.001

[16] C. Cordon-Rosales, D. E. Irwin, J. Li, U. S. Nair, N. Padilla, T. L. Sever, R. M. Welch, Dynamic Malaria Models with Environmental Changes, Proceedings of the Thirty- Fourth Southeastern Symposium on System Theory Huntsville, (2002) 396-400.

[17] F. Courchamp, C. Diagne, R. E. Gozlan, I. Jari, B. Leroy, D. Roiz, J. M. Salles, A. C. Vaissière, High and rising economic costs of biological invasions worldwide, *Nature* 592(2021) 571-576. https://doi.org/10.1038/s41586-021-03405-6.

[18] L. Dan, X. Zhiongyi, On the study of an SEIV epidemic model concerning vaccination and vertical transmission, *Journal of Applied Mathematics and Bioinformatics,* 1(2011) 21-30.

[19] K. Dietz, L. Molineaux, A. Thomas. A malaria model tested in the African savannah, *Bull World Health Organ*, 50(1974) 347-357.

[20] R. Eritja, R. Escosa, J. Lucientes, E. Marques, R. Molina, D. Roiz, S. Ruiz, Worldwide invasion of vector mosquitoes: present European distribution and challenges for Spain, *Biol. Invasions*, 7(2005) 87-97. https://doi.org/10.1007/ S10530-004-9637-6.

[21] M. Ferraguti, A. Ibáñez-Justicia, S. Magallanes, Implication of human landscape transformation on mosquito populations, *Ecology and Control of Vector-Borne Diseases Wageningen Academic Publishers*, 10(2022) 143-160 https://doi.org/10.3920/ 978-90-8686-931-28.

[22] M. U. Ferreira, H. M. Yang. Assessing the effects of global warming and local social and economic conditions on the malaria transmission, *Revista de Saude Publica*, 34(2000) 214-222, doi: 10.1590/S0034-89102000000300002.

[23] J. Figuerola, A. Higueros, T. Montalvo, A. Ortiz, V. Peracho, E. Realp, A. Valsecchi, C. Vila, Effectiveness of the modification of sewers to reduce the reproduction of Culex pipiens and Aedes albopictus in Barcelona, Spain, Pathogens 11 (2022) 423. https://doi.org/10. 3390/PATHOGENS11040423.

[24] W. A. Foster, C. M. Stone, G. C. Walsh, A. B. R. Witt, Would the control of invasive alien plants reduce malaria transmission? A review, *Parasites and Vectors,* 11(2018) 38-76. DOI 10.1186/s13071-018-2644-8.

[25] A. B. Gumel, K. Okuneye, Analysis of temperature and rainfall dependent model for malaria transmission dynamics, *Maths Bios.*, 32(2015) 1-12.

[26] S. Heinz, O. Horstick, A. Kolimenakis, A. Michaelakis, D. Papachristos, C. Richardson, M. L. Wilson, V. Winkler, L. Yakob, The role of urbanisation in the spread of Aedes mosquitoes and the diseases they transmit: a systematic review, *PLoS Negl. Trop. Dis.* 1 (2021)5, e0009631. https://doi.org/10.1371/JOURNAL.PNTD.0009631

[27] Y Higa, Dengue vectors and their spatial distribution, *Trop. Med. Health,* 39(2011), S17-S27. https://doi.org/10.2149/TMH.2011-S04.

[28] S. Junping, S. Ruoyan, Global stability of multigroup epidemic model with group mixing and nonlinear incidence rates, *Appl Math and Comp,* 218 (2011) 280-286, doi: 10.1016/j.amc.2011.05.056.

[29] G. Macdonald, The epidemiology and control of malaria, Oxford University Press, London, 1957

[30] O. D. Makinde, K. O. Okosun, Modelling the impact of drug resistance in malaria transmission and its optimal control analysis, *International Journal of the Physical Sciences,* 6(2011) 6479-6487 doi: 10.5897/IJPS10.542.

[31] S. Mandal, R. R. Sarkar, S. Sinha, Mathematical models of malaria - a review, *Malaria Journal*, 10(2011) 188-202, doi: 10.1186/1475-2875-10-202.

[32] G. A. Ngwa, W. S. Shu, A mathematical model for endemic malaria with variable human and mosquito populations, *Math Comput. Model,* 32(2000) 747-763, doi: 10.1016/S0895-7177(00)00169-2.

[33] A. M. Norberto, S. Vanessa. Modelling the Spatial Spread of Chagas Disease, *Bulletin of Mathematical Biology Springer,* 56(2019) 1-44.

[34] A. Nwankwo, D. Okuonghae, A mathematical model for the population dynamics of malaria with a temperature dependent control. Foundation for Scientific Research and Technological Innovation, *Springer,* 15(2019), 1-30.

[35] R. Ross, The prevention of malaria, John Murray, London, 1911, 23-85.

CHARITY JUMAI ALHASSAN
DEPARTMENT OF MATHEMATICS, EDO STATE UNIVERSITY, UZUAIRUE, AUCHI OKENE ROAD, IYAHMO, EDO, NIGERIA
ORCID: 0000-0002-3213-9512
Email address: joy4r3al@gmail.com

KENNETH OJOTOGBA ACHEMA
DEPARTMENT OF MATHEMATICS, JOSEPH SARWUAN TARKA UNIVERSITY, MAKURDI, NORTH BANK, MAKURDI, 2373, BENUE, NIGERIA
ORCID: 0000-0000-0000-0000
Email address: achema.kenneth@uam.edu.ng